Ligand field and interference effects in L-edge x-ray Raman scattering of MnF_2 and CoF_2

J. Jiménez-Mier*,[a], G.M. Herrera-Pérez[a], P. Olalde-Velasco[a], D.L. Ederer[b], and T. Schuler[b].
[a]*Instituto de Ciencias Nucleares, Universidad Nacional Autónoma de México, 04510 México DF, México.*
[b]*Department of Physics, Tulane University, New Orleans, LA 70118, U.S.A.*

Recibido el 14 de mayo de 2007; aceptado el 26 de octubre de 2007

We present experimental results for x-ray absorption and resonant emission at the L-edge of the transition metal in MnF_2 and CoF_2. The emission data are corrected for self-absorption. The data are compared with calculations in both the free-ion approximation and with the effect of the ligand field of D_{4h} symmetry included. The results of the calculations take into account interference terms in the Kramers-Heisenberg expression. We obtain very good agreement between experiment and theory for both x-ray absorption and resonant emission in the two compounds. The inclusion of the ligand field is important to achieve such agreement. However, the results of the calculation that does not take into account the interference terms are in better agreement with experiment, indicating that the model used probably overestimates the importance of interference effects.

Keywords: x-ray Absorption; x-ray emission; electronic structure; transition metal compounds.

Presentamos resultados experimentales para absorción y emisión resonante de rayos x en la orilla L del metal de transición en MnF_2 y CoF_2. Los datos de emisión se presentan corregidos por autoabsorción. Los datos se comparan con cálculos en la aproximación de ión libre y con el efecto de un campo ligante de simetría D_{4h} incluido. Los resultados del cálculo toman en cuenta los términos de interferencia en la expresión de Kramers-Heisenberg. Se encuentra muy buen acuerdo entre el experimento y la teoría en los dos compuestos. La inclusión del campo ligante es muy importante para alcanzar dicho acuerdo. Sin embargo, los resultados del cálculo que no incluyen los términos de interferencia están en mejor acuerdo con el experimento, indicando que el modelo empleado probablemente sobre-estima la importancia de los términos de interferencia.

Descriptores: absorción de rayos x; emisión de rayos x; estructura electrónica; compuestos de metales de transición.

PACS: 78.70.Ck; 78.70.En

1. Introduction

X-Ray spectroscopies have become major tools to study the electronic structure of complex compounds [1,2]. There are many examples now of their use in the determination of the electronic structure of 3d transition metal compounds. X-Ray absorption spectroscopy in the vicinity of the $L_{2,3}$ edge of the transition metal gives information about the unoccupied states of 3d symmetry that can be reached by electromagnetic excitation of a $2p$ core electron. Normal x-ray emission spectroscopy, which occurs whenever a $2p$ hole is created, gives information about the occupied $3d$ states, but usually of the system with one less electron. Therefore this normal L emission gives information about the electronic states of the ion subject to a strong Coulomb interaction. However, if the production of a $2p$ hole is accompanied by the production of a $3d$ bound state in the transition metal ion and decay is monitored by x-ray emission one gets information about excited states of the system in the same state of ionization as the ground state. One can then obtain information about d-excited states of the valence shell that originate in the interplay between the $3d^n$ atomic multiplet and the electrostatic field due to the ligands. Charge transfer effects are also present in both absorption and resonant emission spectra at the $L_{2,3}$ edge of a transition metal compound. A resonant emission spectrum of a transition metal compound may have an elastic emission peak that results from decay into the $2p$ hole by photon emission of the same energy as the exciting photon. The d to d excited states correspond to emission of x-ray photons whose energy is a few eV less than the energy of the incoming photon. This results in one or several inelastic emission peaks. The energy lost by the photons is then equal to the energy required to produce the d-excited state of the ion. For slightly larger values of the energy loss one then finds charge transfer emission peaks that correspond to decay into states of the form $3d^{n+1}\underline{L}$, where $\underline{L}$ denotes a hole in the ligand and the electron now appears as an extra electron in the $3d$ transition metal subshell.

The interpretation of the x-ray absorption and emission spectra of transition metal compounds is aided by calculations that have been very successful in reproducing the experimental results [1-4]. The calculations must take into account the major interactions in the system. The first one is the structure of the $3d^n$ atomic multiplet that results from the intra-atomic electron-electron Coulomb repulsion. The agreement with experiment is further improved once ligand field effects are included. Charge transfer effects may also be added to the calculation [3,4].

The $3d$ transition metal fluorides are interesting systems in this regard [5-9]. They are certainly the most ionic com-

pounds that one can find, and therefore they should clearly show the effect of both the atomic multiplet and the ligand field. Absorption and resonant emission spectra of transition metal fluorides usually present sharp features compared to the corresponding oxides. Thus they are good candidates for references of absorption and emission spectra of ionic $3d^n$ compounds.

Recently we have published data for x-ray absorption and resonant emission at the $L_{2,3}$ edge in MnF_2[7], FeF_2 [10] and CoF_2 [9]. The results indicate that the x-ray absorption spectrum are very good references for M^{2+} ionic compounds, where M is the transition metal. The corresponding emission spectra can be used to obtain information about the atomic multiplet structure of these compounds, and also about ligand field effects.

In this article we present the x-ray absorption and emission results of calculations that include atomic multiplet and ligand field effects for Mn^{2+} and Co^{2+} ions in D_{4h} symmetry. We also treat the effect due to emission from a polycrystalline sample in which the crystals are randomly oriented. The calculations follow the two-photon expression due Kramers-Heisenberg, and thus contain effects due to interference within the core-excited intermediate state. We also obtain an expression for emission in which interference effects are neglected. The results of these calculations are compared with the experimental data.

2. Experiment

The experiment took place at beamline 8.0 at the Advanced Light Source of Lawrence Berkeley Laboratory. Monochromatized photons from a *5.0 cm* undulator (U5.0) are focused onto the sample, and the resulting emission spectra are recorded with a high efficiency x-ray spectrometer. This soft x-ray fluorescence spectrometer is a grazing incidence instrument with a fixed entrance slit and a position sensitive area detector. A total electron yield (TEY) spectrum is obtained by recording the total electric current through the sample as the energy of the exciting photons is scanned. Photon emission spectra are then recorded at selected values of the incoming photon energy by positioning the spectrometer detector along the Rowland circle to intercept the wavelength region of interest. Details of the beam line and the spectrometer have been published in reference 11, where there is a diagram of the experimental setup. The incoming radiation flux was monitored by the total photocurrent produced in a gold mesh placed in front of the beam just before the sample chamber. The monochromator energy was calibrated with the absorption spectrum of metallic manganese iron, cobalt, nickel and copper samples that cover the entire region between 630 and 940 *eV*. We estimate that this calibration is accurate within *0.3 eV*. The emission energy was then determined by the elastic emission peaks present in several of the spectra. The spectrometer detects photons emitted along the polarization direction of the incoming beam, in the so-called unpolarized geometry [12]. The MnF_2 and CoF_2 samples were commercial powders of purity greater than *99 %*.

The resonant emission occurs in a photon energy region that is strongly affected by self-absorption [13]. We corrected for this effect following the procedure that is described in detail in previous work [7]. Briefly, the emission intensity at the photon energy $h\nu_2$ should be corrected with the expression [7,13]

$$I(h\nu_2) = I_m(h\nu_2)\left[1 + \frac{\mu_o}{\mu_i}\cot\theta\right] \quad (1)$$

where I_m is the measured intensity at the photon energy $h\nu_2$, μ_i is the absorption cross section at the excitation photon energy $h\nu_1$, μ_o is the absorption cross section at the emission photon energy $h\nu_2$, and θ is the angle of incidence of the x-rays with respect to the normal. In our case the sample makes an angle of 45^o. The absorption cross section μ is obtained from our TEY spectra corrected so that the step in the signal from just before the $L_{2,3}$ edge to the continuum absorption above L_2 is equal to the mass absorption coefficient for the compound. Values for the mass absorption coefficients for MnF_2 and CoF_2 were calculated in-line at the Center for X-Ray Optics web page of the Advanced Light Source [14].

Figure 1 gives examples of the effect of the self absorption for resonant emission in both MnF_2 and CoF_2. To the left we show the data for MnF_2 and to the right are the corresponding data for CoF_2. The top panel is the TEY spectrum. The shaded gray in the bottom panel is the uncorrected emission spectrum, and the continuous line gives the result of the self-absorption correction. The value of the excitation energy $h\nu_1$ is indicated by the vertical line in the TEY spectra. The spectrum in MnF_2 illustrates that self-absorption has a rather significant effect whenever there is a weak resonance above the L_3 edge. According to eq. 1, for our detection geometry self-absorption cuts in half elastic emission, but the effect is stronger for emission at the top of the absorption cross section. This is not as important for CoF_2, even though it shifts the peaks toward higher emission energies, and it also modifies the relative emission intensities. All emission spectra shown in this paper are corrected for self-absorption.

3. Atomic Multiplet Ligand Field Calculation

Resonant x-ray absorption and emission is a coherent second order process that is described by the Kramers-Heisenberg expression:

$$\sigma(\nu_1,\nu_2) \propto \sum_{f,g}\left|\sum_i \frac{\langle f|\,\vec{\varepsilon}_2\cdot\vec{r}\,|i\rangle\,\langle i|\,\vec{\varepsilon}_1\cdot\vec{r}\,|g\rangle}{h\nu_1 - (E_i - E_g) - i\Gamma_i/2}\right|^2 \times \delta\left[h(\nu_2-\nu_1) - (E_f - E_g)\right] \quad (2)$$

where $|g\rangle$, $|i\rangle$ and $|f\rangle$ are the initial-, intermediate-, and final-state wavefunctions with energiesE_g, E_i, andE_f respectively. The transition operator $\vec{\varepsilon}\cdot\vec{r}$ assumes that all are electric dipole transitions [15], Γ_i is the $2p$ core hole width and the delta function assures overall conservation of energy. A coherent sum over intermediate (core excited) states and incoherent sums over initial and final states are performed.

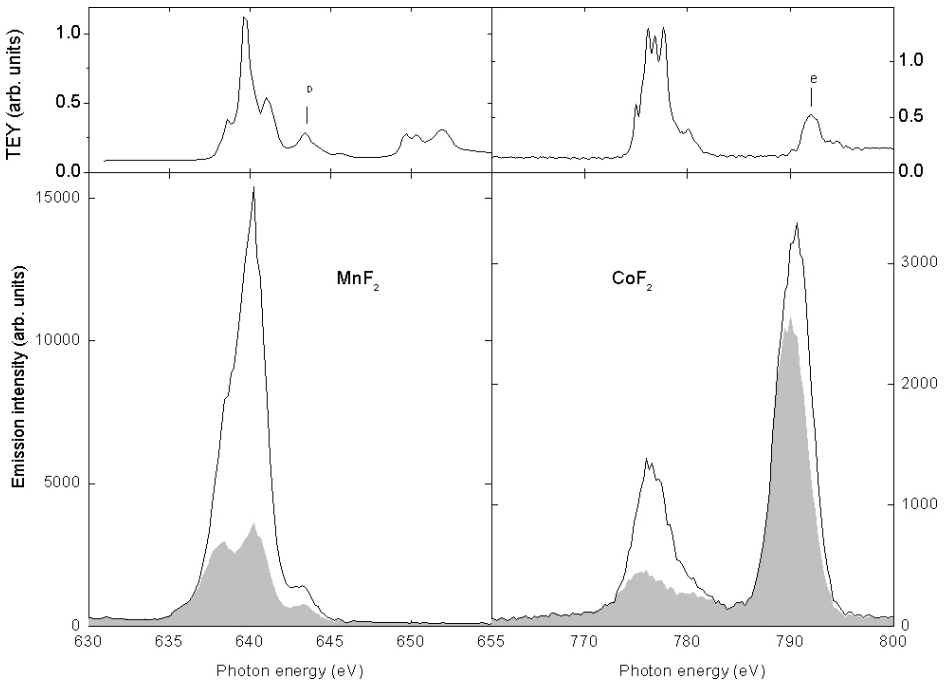

FIGURE 1. Self absorption correction for MnF_2 and CoF_2. Top: TEY spectra with the value of the excitation energy $h\nu_1$ indicated by a vertical line. Bottom: Raw emission spectra in dark gray and corrected emission spectra in solid lines.

In our experiment we have to calculate the convolution of eq. (2) with the monochromator window function $W(h\nu_1 - h\nu_1'; \gamma)$ whose width is γ. The result of this convolution is

$$\sigma(\nu_1,\nu_2) \propto \sum_{f,g} \left| \sum_i \frac{\langle f|\, \varepsilon_2 \cdot r\, |i\rangle \langle i|\, \varepsilon_1 \cdot r\, |g\rangle}{h\nu_2 - (E_i - E_f) - i\Gamma_i/2} \right|^2 \times W\left[h(\nu_2-\nu_1) - (E_g - E_f); \gamma)\right] \quad (3)$$

Both our samples are polycrystalline, and their crystal structure is tetragonal. We incorporate these geometrical effects into this expression. With the polarization vector of the incoming radiation defining the z-axis of our experiment and a fixed detection angle, we consider a single crystal oriented in an arbitrary direction. Both absorption an emission transition matrix elements depend on the relative orientation of the crystal with respect to the polarization vectors ε_1 and ε_2. One has perpendicular or parallel transition matrix elements according to whether ε is parallel or perpendicular to the crystal unequal axis (the c-axis). One then sums over all possible orientations of the crystal. The final expression for the scattering cross section depends on the emission detection direction. It takes a particularly simple form if the detection direction makes the magic angle $\theta_m = 54.7^o$ with respect to the polarization direction of our incoming beam. Even though this does not correspond to our detection geometry, preliminary results show that for our two compounds any effects due to the angular dependence are not greater than a few percent. We therefore feel confident to use the following expression for the scattering cross section:

$$\sigma(\nu_1,\nu_2) \propto \sum_{f,g} \left\{ |S_{12}^{\alpha\alpha}|^2 + 2\left[\left|S_{12}^{\alpha\beta}\right|^2 + \left|S_{12}^{\beta\alpha}\right|^2 + 2\left|S_{12}^{\beta\beta}\right|^2 \right] \right\} \times W\left[h(\nu_2-\nu_1) - (E_g - E_f); \gamma\right] \quad (4)$$

where the coherent sums are given by:

$$S_{12}^{\kappa\lambda} = \sum_i \frac{M_{fi}^{\kappa} M_{ig}^{\lambda}}{h\nu_2 - (E_i - E_f) - i\Gamma/2}$$

the M's are transition matrix elements, κ and λ denote polarization states of the transitions, with α indicating that the polarization vector is parallel to the crystal c-axis and β representing a transition matrix element with polarization vector perpendicular to the crystal c-axis.

If one completely neglects interference effects and performs the square of the transition matrix elements first and then the sum over intermediate states one gets the following expression for the scattering cross section:

$$\sigma(\nu_1,\nu_2) \propto \sum_{f,g,i} \left\{ \frac{\left(\left|M_{ig}^{\alpha}\right|^2 + 2\left|M_{ig}^{\beta}\right|^2\right)\left(\left|M_{fi}^{\alpha}\right|^2 + 2\left|M_{fi}^{\beta}\right|^2\right)}{\left[h\nu_2 - (E_i - E_f)\right]^2 + \Gamma_i^2/4} \right\} \times W\left[h(\nu_2-\nu_1) - (E_g - E_f); \gamma\right] \quad (5)$$

We obtained the wavefunctions and transition matrix elements from a free ion Hartree-Fock calculation [16]. Three parameters $10D_q$, D_s and D_t, are used for the ligand field

calculation in this HF basis [3,4]. The output of this calculation [3,4] is a file with the energy values of the states in the $3d^n$ ground state configuration and in the $2p^5 3d^{n+1}$ core excited configuration. The file also contains [3,4] the matrix elements needed to evaluate eq. 4 and 5. We wrote a computer program that directly compares the calculated absorption intensity with the measured TEY spectrum, and then for each value of the excitation energy it calculates the corresponding emission considering both interference effects (eq. 4) and completely neglecting them (eq. 5). One also has to include values for the core-hole width [17] and the monochromator and spectrometer widths and window functions. For both monochromator and spectrometer windows we used Gaussians. The values of the parameters used in the calculations are given in Table I.

4. Results and discussion

In Fig. 2 we make a comparison between theory and experiment for MnF_2. At the bottom on the left we show the experimental TEY spectrum. The result of the ligand field calculation is in the middle panel, and on top we present the result of an absorption calculation for the free ion, with all ligand field parameters equal to zero. To the right we show emission spectra obtained for excitation energies indicated by D and G in the TEY spectrum and a comparison with the calculated emission spectra for the free ion and the ligand field, both with and without interference.

The free ion calculated absorption already has most of the features observed in the TEY spectrum. However, the experimental splitting is only obtained when one performs the ligand field calculation. For MnF_2 it is enough to use an octahedral field. However, in this work the same data is used for both absorption and emission calculations so we decided to perform them in a D_{4h} tetragonal field that distinguishes parallel and perpendicular transitions.

TABLE I. Ground configuration and parameters used in the calculations. The first three are the D_{4h} ligand field parameters that give the best agreement between the calculated and the measured absorption. The core hole width is from Ref. 17. The monochromator and spectrometer widths are used in final convolutions to compare with experimental data.

	MnF_2	CoF_2
Ground configuration	$3d^5$	$3d^7$
Ground term	^{6}S	^{4}F
Parameter (eV)		
$10D_q$	0.92	0.69
D_s	.030	-.074
D_t	.015	-.007
Core hole width Γ	0.14	0.15
Monochromator width (FWHM) γ	0.22	0.22
Spectrometer width (FWHM)	1.58	1.75

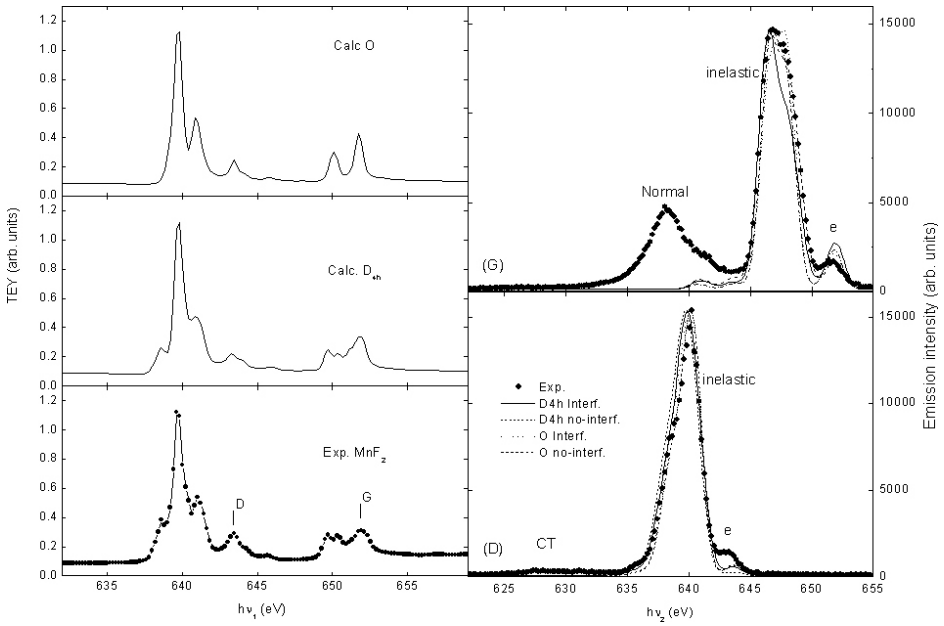

FIGURE 2. Comparison between experiment and theory for MnF_2. Left: absorption spectra. In the bottom there is the experimental TEY spectrum, in the middle there is the calculated absorption with the D_{4h} parameters given in Table I, and on top we show the result of the free ion calculation. D and G are the excitation energies used for the emission spectra. Right: emission spectra obtained at D and G. The dots are the experimental results after self-absorption correction. The lines are the results of the calculations. Continuous line: ligand field with interference; dashed line: ligand field without interference; dotted line: free ion with interference; dotted-dashed line: free ion without interference.

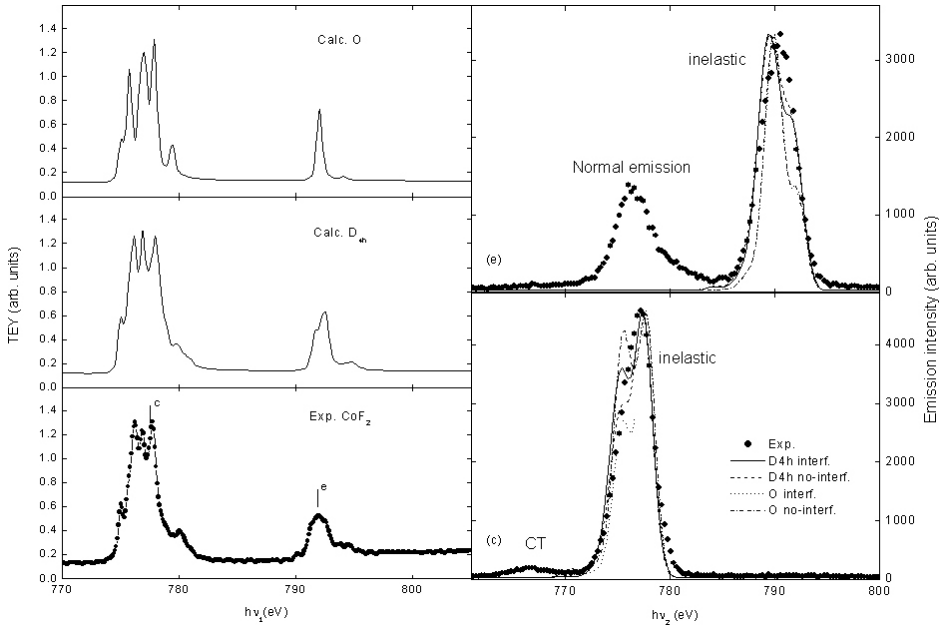

FIGURE 3. Comparison between experiment and theory for CoF_2. Left: absorption spectra. In the bottom there is the experimental TEY spectrum, in the middle there is the calculated absorption with the D_{4h} parameters given in Table I, and on top we show the result of the free ion calculation. c and e are the excitation energies used for the emission spectra. Right: emission spectra obtained at c and e. The dots are the experimental results after self-absorption correction. The lines are the results of the calculations. Continuous line: ligand field with interference; dashed line: ligand field without interference; dotted line: free ion with interference; dotted-dashed line: free ion without interference.

The emission spectrum excited at D is the same we used to illustrate the effect of self-absorption in Fig. 1. It results from excitation at a small resonance group between the main L_3 absorption peak at *640 eV* and the L_2 structure that begins at *649 eV*. There are three emission peaks that correspond to the elastic (e), the inelastic, and a broad, weak charge transfer emission peak indicated by CT in the figure. The only configurations used in the calculation are $3d^n$ and $2p^5 3d^{n+1}$, and therefore the charge transfer peak cannot be reproduced in the calculation. At this excitation energy all theoretical results are in good agreement with the experiment. All predict a small elastic peak and a dominant inelastic peak.

The emission spectrum G results after the resonant production of a $2p_{1/2}$ hole. Here one finds the elastic peak and several inelastic that result from transitions into excited states of the $3d^5$ ground configuration. At about *637 eV* there is a broad peak that results from decay into the $2p_{3/2}$ hole produced non-resonantly. This occurs only for Mn^{3+} ions produced by ionization from the 2p subshell. The calculation does not include this ionic state and therefore cannot reproduce this normal emission peak. Once again, all calculations predict the same overall structure. However, the ligand field calculation without interference is the one that results in the best agreement with theory. The free ion calculations give inelastic peaks that are narrower, and a more intense elastic peak. The ligand field calculation with interference gives a high energy shoulder in the main inelastic peak that is too small.

A similar comparison for CoF_2 is made in Fig. 3. Once again, the absorption spectra are on the left, and two emission spectra are given on the right. The free-ion absorption calculation (top) gives the overall structure, but the best agreement between experiment and theory is for the ligand field calculation. The CoF_2 TEY spectrum presented here shows sharper features compared to the CoO spectrum in ref. [18]. The emission spectra produced by excitation at both L_3 and L_2 edges show what could be considered one broad peak. Comparison with the calculation, however, indicates that for both excitation energies there is a shoulder. In spectrum c the shoulder is on the low energy side and corresponds to inelastic emission. In spectrum e the shoulder is to the high energy side, closer to the elastic emission peak. The free ion calculations predict sharper peaks. The ligand field calculation gives emission peaks of the right width, though the shoulders are not as sharply defined in the experimental data. In both emission spectra the best agreement is found for the ligand field calculation without interference. This is in agreement with the results found for MnF_2.

5. Conclusions

We presented the results of a calculation for x-ray absorption and emission that includes intra-atomic effects due to the atomic multiplet, ligand field effects and also interference in the coherent, two-photon scattering process. Each of these effects can be found in either the absorption or the emission spectra. In particular, effects due to interference in the Kramers-Heisenbegr expression result in significant changes in the calculated emission spectra. The results for Mn^{2+} and Co^{2+} are compared with experimental absorption and emis-

sion spectra of MnF_2 and CoF_2, respectively. Good agreement is found between experiment and theory. In general the best agreement for emission is found for the spectra calculated including ligand field effects but completely neglecting any interference terms.

6. Acknowledgements

We wish to thank Jonathan Denlinger for his expert help at the soft x-ray end station at the ALS. We acknowledge support from DOE-EPSCOR cluster research Grant No. DOE-LEQSF (1993-1995)-03 and from CONACYT México under grant No. U41007-F. The Advanced Light Source is funded by the Office of Basic Energy Science, U.S. Department of Energy Contract No. DE-AC03-76SF00098.

∗. Corresponding author, e-mail: jimenez@nucleares.unam.mx.

1. A. Kotani, *Eur. Phys. J. B* **47** (2005) 3.
2. A. Kotani and S. Shin, *Rev. Mod. Phys.* **73** (2001) 203.
3. F.M.F. de Groot, *Chemical Reviews* **101** (2001) 1779.
4. F.M.F. de Groot, *Coordination Chemistry Reviews* **249** (2005) 31.
5. J. Jiménez-Mier, D.L. Ederer, and T. Schuler, *Phys. Rev. A* **68** (2003) 042715.
6. J. Jiménez-Mier, D.L. Ederer, and T. Schuler, *Phys. Rev. B* **70** (2004) 035216.
7. J. Jiménez-Mier, D.L. Ederer, and T. Schuler, *Phys. Rev. A* **72** (2005) 052502.
8. J. Jiménez-Mier, D.L. Ederer, and T. Schuler, *Radiat. Phys. and Chem.* **75** (2006) 1666.
9. J. Jiménez-Mier *et al.*, *Rev. Mex. Fís. S* **53** (2007) 38.
10. J. Jiménez-Mier *et al.*, *Radiation Effects and Defects in Solids* **162** (2007) 613.
11. J. Jia *et al.*, *Rev. Sci. Instrum.* **66** (1995) 1394.
12. Y. Harada and S. Shin, *J. Electron Spectrosc. Relat. Phenom.* **136** (2004) 143.
13. D.R. Muller *et al.*, *Phys. Rev. B* **54** (1996) 15034; http://www-cxro.lbl.gov/
14. J. Jiménez-Mier, D.L. Ederer, and T. Schuler, *J. Phys. B* **36** (2003) L173.
15. R.D. Cowan, *The Theory of Atomic Structure and Spectra* (University of California Press, Berkeley, 1981).
16. M.O. Krause, *J. Phys. Chem. Ref. Data* **8** (1979) 307.
17. M. Magnuson, S.M. Butorin, J.-H. Guo and J. Nordgren, *Phys. Rev. B* **65** (2002) 205106.